JOURNAL OF MATERIALS SCIENCE 37 (2002) 4445–4450

Crystallization and phase transformation behaviour of electroless nickel-phosphorus deposits with low and medium phosphorus contents under continuous heating

K. G. KEONG, W. SHA, S. MALINOV
School of Civil Engineering, The Queen's University of Belfast, Belfast BT7 1NN, UK
E-mail: w.sha@qub.ac.uk

Electroless nickel-phosphorus deposits with 5–8 wt% P and 3–5 wt% P were analysed for the effects of continuous heating on the crystallization kinetics and phase transformation behaviour of the deposits. The as-deposited coatings consist of a mixture of amorphous and microcrystalline nickel phases, featuring in their X-ray diffraction patterns. Continuous heating processes to 300°C–800°C at 20°C/min were carried out on the deposits in a differential scanning calorimetric apparatus. The subsequent X-ray diffraction analyses show that the sequence of phase transformation process was: amorphous phase + microcrystalline nickel → f.c.c. nickel + Ni_3P stable phases. Preferred orientation of nickel {200} plane developed in the deposits after the heating processes. Differential scanning calorimetry of the deposits indicates that the crystallization temperatures increased with decreasing phosphorus content, and increasing heating rate. Crystallization activation energies of the deposits (230 and 322 kJ/mol, respectively) were calculated using the peak temperatures of crystallization process, from the differential scanning calorimetric curves at the heating rates ranging from 5 to 50°C/min. It was found that the deposit with lower phosphorus content has higher activation energy.

1. Introduction

It was generally reported that the electroless nickel-phosphorus (Ni-P) deposits at as-deposited condition have a non-equilibrium phase structure, which is thermodynamically unstable and would transform into equilibrium state through crystallisation reactions [1–5]. Since the first discovery by Brenner and Riddell in 1944 [6, 7], various investigators have reported that the microstructural properties and crystallization behaviour of electroless Ni-P deposits depend on the phosphorus contents and heating processes of the deposits. However, many conflicting results have been reported from these studies [8–27]. In general, the electroless Ni-P deposits can be classified as low (1–5 wt% P), medium (5–8 wt% P) and high (9 wt% P and more) phosphorus deposits based on their phosphorus contents [28]. Studies have shown that the as-deposited low-phosphorus deposits consist of microcrystalline nickel [22] or crystalline phase [17, 23]. The as-deposited medium-phosphorus deposits can be either amorphous [23] or mixtures of amorphous and microcrystalline nickel phases [8, 17, 24, 26]. At as-deposited condition, the high-phosphorus deposits are reported as amorphous [11, 14, 15, 17, 25], mixtures of amorphous and microcrystalline nickel [13, 21], or those mixtures plus various other intermediate phases like Ni_5P_2, Ni_5P_4 and $Ni_{12}P_5$ [12]. Reports on the effects of phosphorus content and heating processes to the crystallization behaviour of electroless Ni-P deposits were made after various studies by different investigators. Study on the deposits with phosphorus content of less than 7 wt%, using differential scanning calorimetry (DSC) and transmission electron microscopy (TEM), has shown that the deposits transform directly into final Ni_3P stable phase in a matrix of crystalline nickel [16]. Study using DSC and X-ray diffraction (XRD) analyses has shown that the deposits with 4.35–9.1 wt% P transformed into the Ni_3P stable phase during heat treatment, without the precipitation of intermediate phases [8]. However, another study has indicated that the transformation process was accompanied by the formation of intermediate phases like Ni_7P_3 and Ni_5P_2 [20]. Also, a XRD study on the deposit with 8.43 wt% P has shown the presence of metastable Ni_5P_2 and $Ni_{12}P_5$ in addition to the Ni_3P phase [3]. Randin *et al.* has reported that the electroless Ni-P deposits after heating processes consisted of nickel and Ni_3P only [19]. Effects of the heating processes and phosphorus contents on the crystallization temperature of the electroless Ni-P deposits are reported in Refs. [1] and [21]. Study on the deposits with 5.3–11 wt% P has shown that the crystallization temperatures of the deposits decrease with increasing phosphorus level [1]. The crystallization temperatures of the deposits with 7.4–10 wt% P was reported to

have increased with increasing heating rate, but independent of phosphorus content [21]. In Ref. [27], the effect of phosphorus content on the crystallization activation energy of electroless Ni-P (2–12 wt%) deposits was reported. The low-phosphorus deposit has the highest crystallization activation energy, whereas comparison between the medium and high-phosphorus deposits shows that the increase of crystallization activation energy could also result from the increase of phosphorus content. However, similar comparison between coatings with medium (6–9 wt%) and high (10–14 wt%) phosphorus deposits in Refs. [25, 26] respectively, did not confirm the tendency given in Ref. [27].

In the present work, the DSC and XRD analyses have been conducted on the electroless Ni-P deposits with low and medium-phosphorus contents, to investigate the effects of phosphorus content and continuous heating processes on the crystallization kinetics and phase transformation behaviour of the deposits.

2. Experimental procedures

The electroless Ni-P samples used in this work were provided by *Lea Manufacturing Company* in England. The coated-deposit of the medium-phosphorus (MP) sample was nominally 75 μm thick and has 5–8 wt% phosphorus content. The low-phosphorus (LP) sample was nominally 100 μm thick and has 3–5 wt% phosphorus content. Both the samples were deposited on mild steel substrates. To facilitate the heating experiments in DSC apparatus, the samples (coated-deposit and substrate) were cut into small pieces of size 3.5 mm × 3.5 mm, cleaned with methanol and acetone, and rinsed with cold water.

The continuous heating processes were performed using a Netzsch series DSC-404 differential scanning calorimeter at the constant heating rates. Different heating rates were applied, namely 5, 10, 15, 20, 30, 40 and 50°C/min. The sample specimens were placed in a ceramic crucible, and the experiments were carried out in a helium (He) flow (30 ml/min) in the pre-vacuumed DSC heating chamber. An empty crucible of the same kind was used as a reference throughout the experiments. For the XRD analyses, the sample specimens were first heated in the DSC apparatus at a constant heating rate of 20°C/min, up to the temperatures ranging from 300°C–800°C. The subsequently cooled specimens were then scanned at the ambient temperature using a Siemens diffractometer applying Cu $K_{\alpha 1+\alpha 2}$ radiation. The scanned angles (2θ) ranged from 3° to 110°, with a step size of 0.04° and counting time of 1 sec/step. *ProFit*, a computer programme that employed the least squares profile separation fitting technique [29], was used to calculate the integrated intensities of individual phases from the XRD profiles.

3. Results and discussion

3.1. Calorimetric study

The DSC curves of the MP (5–8 wt% P) and LP (3–5 wt% P) samples at different heating rates from 5–50°C/min are shown in Fig. 1a and b. Crystallization peak temperatures (T_m) of the MP and LP samples determined from the major exothermic peaks of the DSC curves were 332°C–362°C and 386°C–408°C, respectively. The results demonstrated that the sample with lower phosphorus content has a higher crystallisation temperature. In the MP sample, there was a shoulder (secondary peak) after the major exothermic peak in the DSC curves (*see* Fig. 1a). The presence of these shoulders in the DSC curves indicates the final stage of crystallisation process, or the relaxation of lattice strain

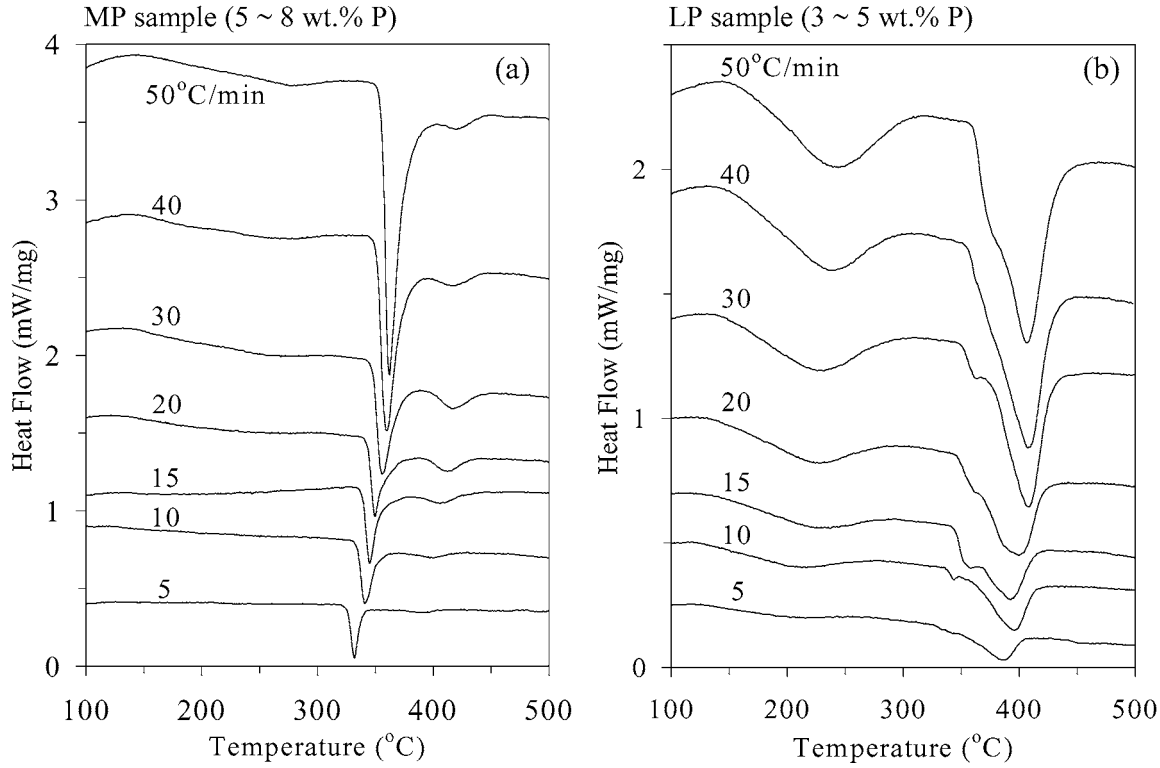

Figure 1 DSC curves of the (a) medium and (b) low-phosphorus samples at the heating rates of 5 to 50°C/min. For the sake of clarity the calorimetric curves were shifted arbitrarily on the vertical scale.

energy during phase separation [21]. In the LP sample, the DSC curves show a small exotherm between 150°C and 300°C. The presence of small exotherm before the major crystallization exothermic peak was also reported in the deposit with 5–6 wt% P [24]. It was reported by the investigators that the small exotherm was related to the release of microstrain, associated with microstructural changes before the major crystallization reaction. As in the MP sample, there was also a shoulder, but this time right before the major exothermic peak in the DSC curves (*see* Fig. 1b). The formation of these shoulders might be related to the short-range atomic movements and incipient crystallisation of metastable crystalline phases [14, 21, 24]. The major exothermic peak in the DSC curves corresponded to the long-range atomic movements causing precipitation of the stable phases such as f.c.c. nickel and Ni_3P [21]. In both samples, the onset and end temperatures of major exothermic peak in some DSC curves were difficult to determine due to the peak overlapping. From Fig. 1, it is also clear that the exothermic temperatures of the major crystallization processes in both samples have increased with increasing heating rates.

Crystallization activation energies of the deposits were calculated using the peak temperatures (T_m) of the crystallisation process at different heating rates (ϕ). Plots of $\ln(T_m^2/\phi)$ versus $1000/RT_m$ from the Kissinger method [30] yield the crystallisation activation energies of 230 ± 6 kJ/mol and 322 ± 54 kJ/mol, respectively, for the MP and LP deposits. These values are close to the self-diffusion activation energy of nickel (289 kJ/mol) [31]. However, the sample with lower phosphorus content has higher crystallization activation energy. This is in agreement with the result reported in Ref. [27] on the low and medium phosphorus deposits.

3.2. X-ray diffraction analysis

X-ray diffraction of the MP (5–8 wt% P) and LP (3–5 wt% P) deposits shown in Figs 2 and 3 indicated that the deposits were the mixture of amorphous and microcrystalline nickel phases in as-deposited condition. The results agreed with the studies from some other investigators showing that both the as-deposited medium [8, 17, 24] and low [22] phosphorus deposits consisted of a semi-amorphous structure. In the present study, the reflections that correspond to the 2θ region of nickel {111} and {200} planes are seen in the XRD

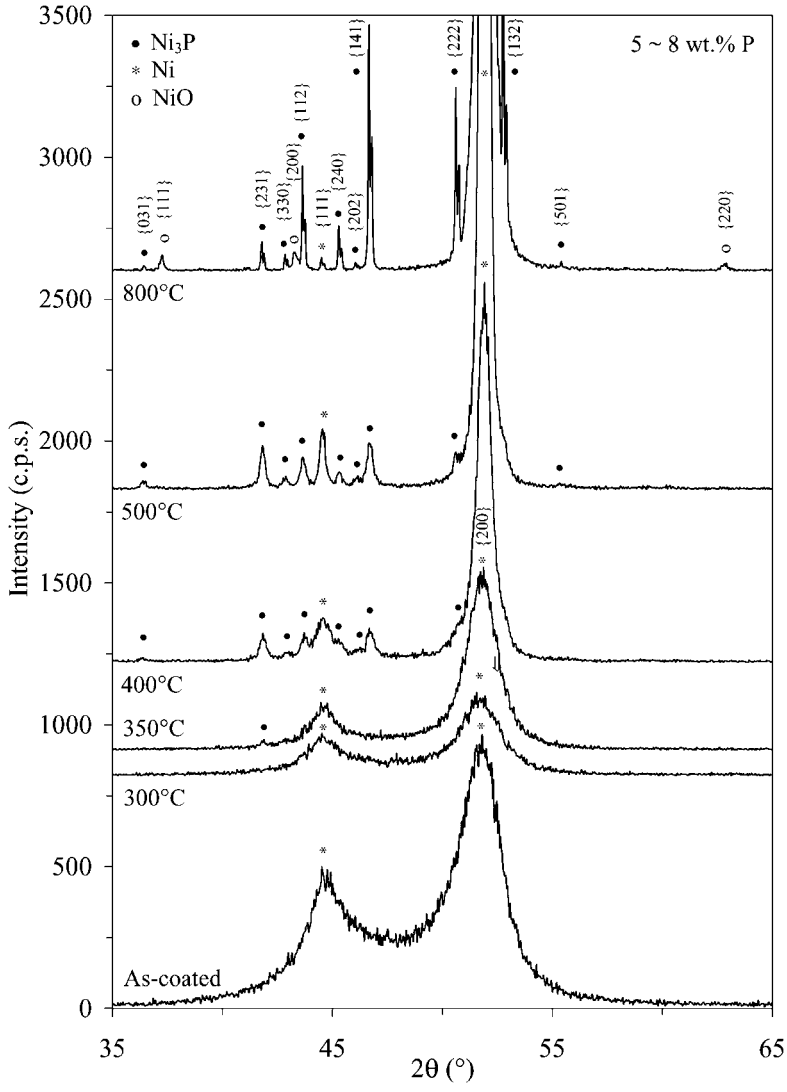

Figure 2 XRD patterns of the electroless Ni-P deposit with 5–8 wt% P (MP sample) at as-deposited condition and after heating at 20°C/min to the end temperatures 300°C–800°C. For the sake of clarity the XRD profiles were shifted arbitrarily on the vertical scale.

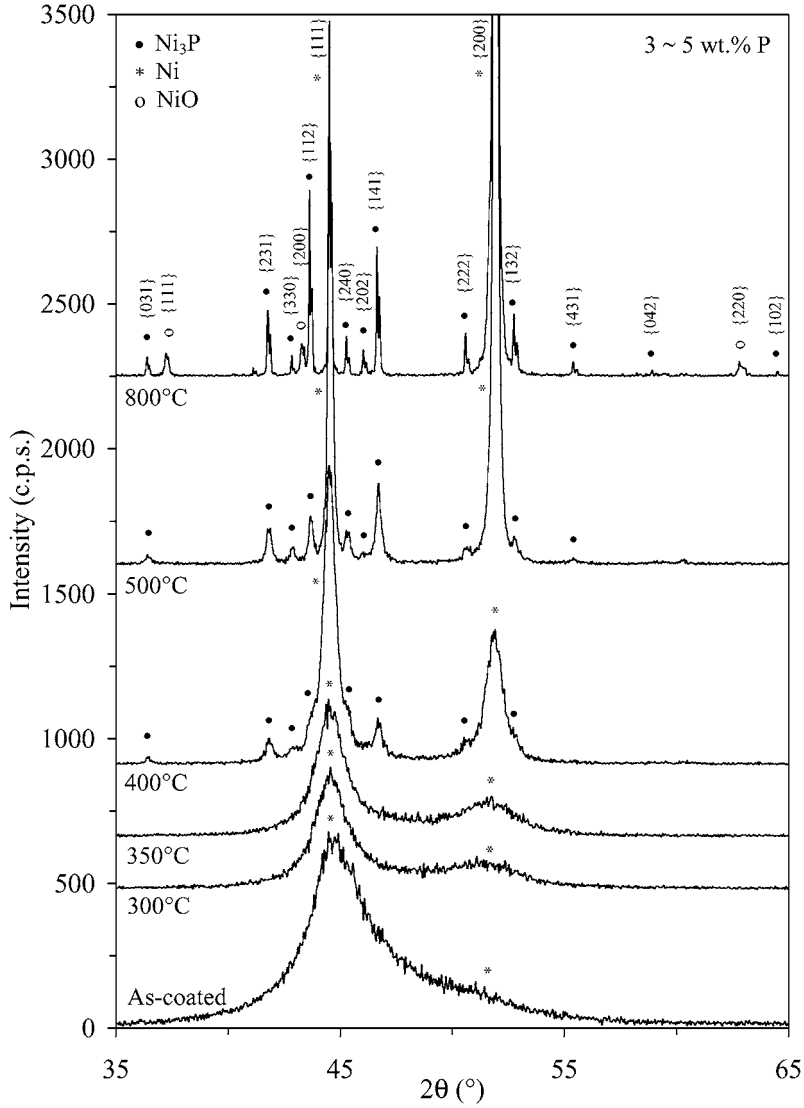

Figure 3 XRD patterns of the electroless Ni-P deposit with 3–5 wt% P (LP sample) at as-deposited condition and after heating at 20°C/min to the end temperatures 300°C–800°C. For the sake of clarity the XRD profiles were shifted arbitrarily on the vertical scale.

profiles. The amorphous profile in both deposits was located between the nickel {111} and {200} reflections. The intensity of nickel {200} reflection in the MP deposit however was higher than the {111} reflection. The preferred orientation was probably predetermined by the initial phosphorus content of the deposit. This contradicted with the opinion that the preferred orientation of nickel phase tends to disappear with increasing phosphorus content in the deposits [21].

In the MP deposit, heating to 300°C at the heating rate of 20°C/min brought small effect on the nickel {111} and {200} deflections (*see* Fig. 2). There was emergence of nickel {311} reflection at 92.9° (2θ). After heating to 350°C, the nickel {200} reflection became sharper and considerably increasing intensity. There was also the Ni_3P {231} reflection in the XRD profile. The phase transformation process was at the expense of the amorphous phase. The major exothermic peak ($T_m = 349$°C) in the DSC curve measured at the same heating rate (20°C/min) was related to these (*see* Fig. 1a). Heating to 400°C leads to further sharpening and intensifying of the nickel {200} reflection, and precipitation of nickel phosphide, Ni_3P, in the 2θ region around the nickel {111} reflection. The further growth of nickel phase and formation of Ni_3P could be related to the small exotherm (shoulder, onset at about 400°C) found in the DSC curve measured at 20°C/min. The emergence of the Ni_3P phase in the deposit also relates to the crystallisation process. However, a small amount of amorphous phase remains in the deposit after the heating process. In Ref. [24] no amorphous phase was found in the medium phosphorous deposit (5–6 wt%) that was heat treated at 400°C isothermally for 60 min. After heating to 500°C, the nickel and Ni_3P reflections further sharpened and strengthened into well-defined diffraction peaks. However, the reflections from the Ni_3P phase were considerably wide and short compared to the nickel reflections, indicating that further refinement of phase reflections is likely at higher temperatures. Numerous minor reflections from the Ni_3P phase were also found in the XRD profile at this heating condition. There was still a relatively small fraction of amorphous phase in the deposit as identified after profile fitting, but it was not obvious when viewing the diffraction pattern. The deposit was suggested as near to complete crystallisation. After heating to 800°C, the nickel and Ni_3P reflections further refined and intensified into narrower and sharper peaks. No amorphous phase remains after

the heating process, indicating complete crystallisation process in the deposit. In addition, a small number of nickel oxide (NiO) reflections were also found in the XRD profile, indicating the presence of oxygen in the DSC heating chamber. The nickel {200} reflection stays as the strongest reflection throughout the heating processes.

In the LP deposit, heating at the heating rate of 20°C/min to the temperature 300°C slightly sharpened the nickel {111} and {200} reflections (*see* Fig. 3). This could be related to the small exotherm (at about 240°C) in the DSC curve measured at the same heating rate (*see* Fig. 1b). In addition, the nickel {311} and {222} deflections were also found at the higher 2θ values. After heating to 350°C, the nickel reflections were slightly further strengthened, but no new phases have been observed so far. Heating to 400°C shows considerable strengthening and sharpening of the nickel {111} and {200} reflections. The reflections from Ni_3P phase were also observed, but most were shadows by the overlapped strengthened nickel reflection. The formation of Ni_3P phase in the deposit also indicates the ongoing of major crystallisation process. This agrees with the major exothermic peak in the DSC curve that was measured at the same heating rate. The amorphous phase remains, but only in a relatively small amount. After heating to 500°C, the nickel and Ni_3P reflections have further sharpened. The nickel {200} reflection became the strongest but at the expense of the nickel {111} reflection. The number of Ni_3P reflections has also increased, but they are considerably short and wide. The transformation of amorphous phase into the crystalline phases has nearly completed. Heating to 800°C has further sharpened and strengthened the nickel and Ni_3P reflections. The Ni_3P reflections became narrow and increase in numbers. As in the MP deposit, the presence of oxygen in the heating process was manifested by the observed NiO reflections in the XRD profile. Complete crystallisation process in the deposit has been achieved after the heating process.

The heating processes did not affect the preferred orientation of the MP deposit. The nickel {200} reflection remains as the strongest peak throughout the heating processes. In the LP deposit, however, preferred orientation of nickel {111} plane maintains at the temperatures to 400°C, but it switched to the nickel {200} after the heating to 500°C. This phenomenon could be explained with different degrees of lattice disorder due to the difference in phosphorus content and heating end temperatures.

3.3. Integrated intensity ratio

The calculated integrated intensities of individual phases—amorphous, nickel and Ni_3P phases, determined from the X-ray reflections of the MP and LP deposits using the computer program *Pro-Fit*, were used to calculate the ratios of integrated intensity of the individual phases, to the total integrated intensity. The relative proportion of the amorphous phase remaining in the deposit, shown by the ratio of the integrated intensity of amorphous phase (I_A) to the total integrated intensity (I_{Total}), could be used to estimate the degree of

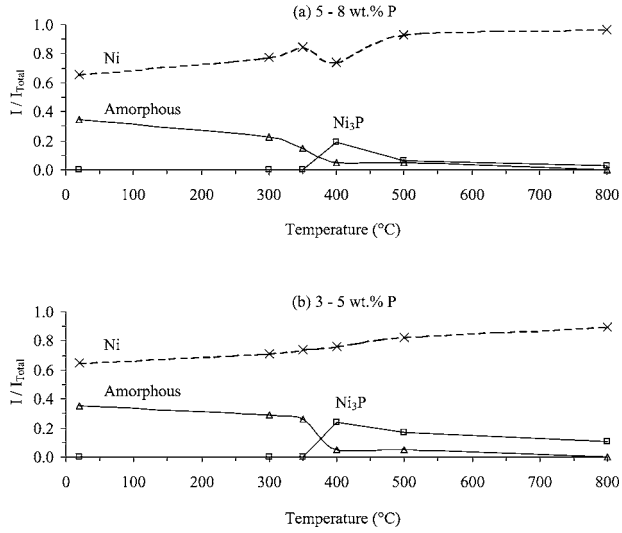

Figure 4 Variation of integrated intensity ratio (I/I_{Total}) with heating temperature of the (a) medium-phosphorus and (b) low-phosphorus deposits.

phase transformation of the deposit over the heating end temperature (Fig. 4). As shown in Fig. 4, the integrated intensity ratios of the amorphous phase (I_A/I_{Total}) in the two samples decreased very gradually to the temperature at 300°C, indicating the absence of major crystallization reactions. From 300°C to 400°C, the ratio of I_A/I_{Total} in both samples dropped to a very low level, due to the ongoing major crystallization reactions at this temperature range. The ratio of $I_{\text{Ni3P}}/I_{\text{Total}}$ has also increased sharply from 350°C to 400°C due to the formation of Ni_3P phase. From 400°C to 800°C, the ratio of I_A/I_{Total} in both samples further reduced to zero, a sign of the complete crystallization process. In both samples, the f.c.c. nickel was the dominant phase from the beginning to the complete crystallization process (*see* Fig. 4). The amount of nickel phase increased at the expense of the amorphous and Ni_3P phases in the deposits.

4. Conclusion

The DSC and XRD studies on the electroless Ni-P deposits with medium and low phosphorus contents in the present work have brought about the following conclusions:

1. At as deposited condition, the medium (5–8 wt% P) and low phosphorus (3–5 wt% P) deposits were the mixture of amorphous and microcrystalline nickel phases.
2. The preferred orientations of the deposits were affected by phosphorus content. The preferred orientation of the low-phosphorus deposit also changed by the heating process.
3. The crystallization temperatures of the deposits increased with decreasing phosphorus content and increasing heating rate.
4. Activation energy of the deposit with low-phosphorus content was higher.
5. The sequence of phase transformation of the deposits was: amorphous phase + microcrystalline nickel → stable microstructure of the f.c.c. nickel and Ni_3P stable phases.

Acknowledgement

Special thank to Mr. R. Laughton (technical manager) of *Lea Manufacturing* in the UK, for useful technical advices and for providing the nickel-phosphorus samples.

References

1. M. W. MAHONEY and P. J. DYNES, *Scr. Metall.* **19** (1985) 539.
2. K. SUGITA and N. UENO, *J. Electrochem. Sci. Technol.* **131** (1984) 111.
3. M. H. STAIA, E. S. PUCHI, G. CASTRO, F. O. RAMIREZ and D. B. LEWIS, *Thin Solid Films* **355–356** (1999) 472.
4. S. V. S. TYAGI, V. K. TANDON and S. RAY, *Z. Metallkd.* **76** (1985) 492.
5. R. N. DUNCAN, *Plat. Surf. Finish.* **83** (1996) 65.
6. A. BRENNER and G. RIDDELL, *J. Res. Nat. Bur. Stand.* **37** (1946) 31.
7. *Idem.*, *ibid.* **39** (1947) 385.
8. P. S. KUMAR and P. K. NAIR, *J. Mater. Process. Technol.* **56** (1996) 511.
9. S. L. CHOW, N. E. HEDGECOCK, M. SCHIESINGER and J. REZEK, *J. Electrochem. Soc.* **119** (1972) 1614.
10. A. H. GRAHAM, R. W. LINDSAY and H. J. READ, *ibid.* **112** (1965) 401.
11. A. W. GOLDSTEIN, W. ROSTOKER, F. SCHOSSBERGER and G. GUTZEIT, *ibid.* **104** (1957) 104.
12. R. C. AGARWALA and S. RAY, *Z. Metallkd.* **79** (1988) 472.
13. S. V. S. TYAGI, V. K. TANDON and S. RAY, *Bull. Mater. Sci.* **8** (1986) 433.
14. E. M. MA, S. F. LUO and P. X. LI, *Thin Solid Films* **166** (1988) 273.
15. E. VAFAEI-MAKHSOOS, E. L. THOSMAS and L. E. TOTH, *Metall. Trans.* **9A** (1978) 1449.
16. K. H. HUR, J. H. JEONG and D. N. LEE, *J. Mater. Sci.* **25** (1990) 2573.
17. N. M. MARTYAK, *Chem. Mater.* **6** (1994) 1667.
18. R. C. AGARWALA and S. RAY, *Z. Metallkd.* **83** (1992) 199.
19. J. P. RANDIN, P. A. MAIRE, E. SAURER and H. E. HINTERMANN, *J. Electrochem. Soc.* **114** (1967) 442.
20. A. CZIRAKI, B. FOGARASSY, I. BOKONYI, K. TOMPA, T. BAGI and Z. HEGEDUS, "Investigation of Chemically Deposited and Electroplated Amorphous Ni-P Alloys" (Central Research Institute for Physics, Budapest, 1980).
21. S. H. PARK and D. N. LEE, *J. Mater. Sci.* **23** (1988) 1643.
22. M. R. LAMBERT and D. J. DUQUETTE, *Thin Solid Films* **177** (1989) 207.
23. Q. X. MAI, R. D. DANIELS and H. B. HARPALANI, *ibid.* **166** (1988) 235.
24. N. M. MARTYAK and K. DRAKE, *J. Alloy. Compd.* **312** (2000) 30.
25. K. G. KEONG, W. SHA and S. MALINOV, *ibid.* **334** (2002) 192.
26. *Idem.*, *Acta Metall. Sin. (Eng. Lett.)* **14** (2001) 419.
27. N. M. MARTYAK, S. WETTERER, L. HARRISON and M. MCNEIL, *Metal Finish.* **92** (1994) 111.
28. Y. Z. ZHANG, K. ZHANG, J. H. FAN and S. M. ZHANG, *Trans. Nonferrous Met. Soc. China* **8** (1998) 642.
29. B. GRZETA and H. TORAYA, *Croat. Chem. Acta* **67** (1994) 273.
30. H. E. KISSINGER, *Anal. Chem.* **29** (1957) 1702.
31. D. S. WILKINSON, in "Mass Transport in Solids and Fluids" (Cambridge University Press, Cambridge, 2000) p. 242.

Received 21 September 2001
and accepted 17 April 2002